THE UNIVERSITY OF CHICAGO

DEADLINE-BASED GRID RESOURCE SELECTION FOR URGENT COMPUTING

A THESIS SUBMITTED TO
THE FACULTY OF THE DIVISION OF THE PHYSICAL SCIENCES
IN CANDIDACY FOR THE DEGREE OF
MASTER OF SCIENCE

DEPARTMENT OF COMPUTER SCIENCE

BY

NICK TREBON

CHICAGO, ILLINOIS

JUNE 2008

Abstract

Scientific simulation and modeling often aid in making critical decisions in such diverse fields as city planning, severe weather prediction, and influenza modeling. In some of these situations, the decisions must be made before a strict deadline, after which the results are of little use. Therefore, it is imperative that these *urgent computations* begin execution as quickly as possible. The Special PRiority and Urgent Computing Environment (SPRUCE) aims to provide faster access to computational Grid resources for urgent computations. Participating Grid resources define local policies that dictate how urgent computing jobs are handled. For instance, some resources may kill currently running jobs to allow immediate access, whereas other resources may only grant next-to-run status. However, the user is still faced with the challenging problem of resource selection. In particular, the user must select the *configuration* (i.e., specification of the computational resource, data repositories, urgent computing policy and runtime parameters) that will provide the highest probability of meeting the desired deadline. The purpose of this thesis is to present and evaluate a set of methodologies and heuristics that generate empirically based, probabilistic upper bounds for the total turnaround time (i.e., file staging, batch queue, and execution delay) for urgent computations. These upper bounds may then be used to guide the user in selecting a configuration that offers the greatest probability of meeting a given deadline. Also provided to guide the user is supplemental data, such as the current queue state at each resource and the historical reliability of the computation at a given resource.

Chapter 1

Introduction

Scientific simulation and analysis are often used to guide critical decisions. For example, global climate modeling influenced the development of the Kyoto protocol [1]. Another example is the use of computerized models to aid cities in planning new freeways or to ease congestion [2]. These examples highlight the importance of scientific simulation and modeling in the decision-making process. However, both these examples exhibit little urgency in obtaining the results from a computer simulation. In contrast to these examples is a domain of problems in which there exists only a brief decision-making window that operates under strict deadlines. Often, in this domain of *urgent computing*, late results are useless results. For instance, a tornado modeling application must provide accurate results with enough warning that the residents in the target area can seek shelter. Similar situations occur in scenarios involving wildfires, hurricanes, and tracking of urban airflow contaminants. In order to meet the deadlines, it is necessary for such urgent computations to access Grid resources easily and quickly.

The Special PRiority and Urgent Computing Environment (SPRUCE) [3, 4] is a token-based framework that enables these high-priority urgent computations to efficiently access Grid resources with elevated priorities. Computational resources that participate are given the flexibility to decide locally how they will respond to urgent computation requests. However, the problem of resource selection is left to the user. The user's primary concern is completing the urgent computation prior to the deadline. One method to determine the feasibility of meeting the deadline is to generate a probabilistic upper bound on the total turnaround time, which consists of the delay incurred for any file staging (both input and output), the resource allocation delay (i.e., batch queue delay), and the execution delay.

This thesis introduces a set of methodologies and heuristics that, taken together, seek to generate a probabilistic upper bound for a *configuration*—in other words, a specification of the data repositories, computational resource, runtime parameters and policy. These methodologies and heuristics are included as part of the *Advisor*, a prototype of a tool that aims to guide an urgent computing user in resource selection. The Advisor also presents supplementary data, such as the current queue state of each resource and the historical reliability of the given application on each resource, that may further aid the user in selecting a resource with greater confidence that the computation will complete prior to the deadline.

The remainder of this thesis is organized as follows. In Chapter 2, a literature review of related work is presented. Chapter 3 introduces the SPRUCE framework, which serves as the context for this work. In Chapter 4, the methodologies and heuristics that make up the Advisor implementation are introduced. Chapter 5 describes a series of experiments that demonstrate the correctness and utility of the upper bounds for a case study application. Conclusions are presented in Chapter 6 and future work is detailed in Chapter 7.

Chapter 2

Literature Review

Many current approaches to the Grid resource selection problem seek to reduce the total turnaround time (or more simply, some aspect of the total turnaround time such as execution delay or communication cost). However, these approaches are not suitable for urgent computing. In this domain, there is often little utility in initiating a computation if a deadline cannot be met. Thus, reducing the total turnaround time does not directly answer the question of whether the deadline is feasible. Furthermore, the traditional Grid resource selection problem is complicated by the fact that each resource may have multiple policies in place for handling urgent requests (e.g., promoting the job to next-to-run status, preemption) that depend on the urgency level of the computation in question. These policies will directly affect how long an urgent computation waits in a batch queue and, thus, the probability of meeting a given deadline. In many cases, these policies represent new mechanisms at a given resource, resulting in a lack of statistical data on which to generate probabilistic bounds. In addition, accurate techniques for bounding the delay for these policies are necessary despite the fact that actual occurrences of urgent computing events utilizing these policies may be rare. The remainder of this chapter presents an overview of a few of the current approaches to the general Grid resource selection problem and how they can be used to help solve the resource selection problem for urgent computing.

Schopf [5] presents a brief overview of the tasks a Grid resource scheduler should perform. The tasks are separated into three classes: resource discovery, system selection and job execution. Resource discovery includes determining the subset of machines the given user has authorization for that also meet the minimum necessary job requirements (e.g., OS, RAM, connectivity, disk space). SPRUCE explicitly handles this step with a warm standby mechanism, which is discussed in Chapter 3.1. System selection tasks consist of gathering dynamic information and selecting a system based on this information. This is exactly the functionality that the Advisor provides. Additionally, the Advisor ranks the resources and configurations by the probability of meeting the deadline. The final stage is execution, which includes advance reservation, job submission, preparation, monitoring, job completion and cleanup. Currently, the Advisor is not responsible for scheduling the urgent computations. Rather, it simply guides the user in resource selection. Schopf raises an issue about scheduling that SPRUCE should consider: What if the submitted application is not achieving the predicted performance? One solution is speculative execution (i.e., submitting the job to multiple resources). Once one copy begins execution, the remaining jobs can be killed or allowed to complete execution for reliability. While not explicitly part of the Advisor's functionality, a poorly performing urgent application may result in a reinvocation of the Advisor to select a new resource on which to run. Thus, the Advisor may be invoked repeatedly.

One approach in Grid resource scheduling is a reputation-based methodology adapted from the P2P EigenTrust algorithm [6]. Here, entities on the Grid (e.g., users, resources, or services) have a reputation and trust value associated with them. The reputation is based on past behavior; the trust value is calculated by examining the trust of the institution that owns the entity and the trust value of the entity based on the contexts it supports. The incorporation of reputation and trust serve to avoid underprovisioned and malicious resources. In the setting of urgent computing, high levels of trust and reputation are implicit. The set of resources for a given application is predetermined. In fact, SPRUCE's warm standby mechanism requires that each potential resource for a given urgent application already have a debugged and tuned version of that application. Furthermore, the application will have a validation history of past performance on each resource. Thus, the problem of a malicious entity is not a concern in the SPRUCE context.

The *matchmaking* and *ClassAds* framework employed by Condor [7] attempts to pair resource requests with matching resources through a classified ads approach [8]. In particular, resources advertise their characteristics, and users advertise their requests. The matchmaker attempts to find matches between these advertisements. The matchmaker framework attempts to solve some of the problems that occur when trying to apply traditional resource management techniques to high-throughput environments (i.e., environments where resources are distributively owned and heterogeneous). In SPRUCE, the warm standby resources are the potential matches – the Advisor needs only to rank them based on both real-time and historical data. The matchmaker has a ranking feature that evaluates some rank function for each resource. For the Advisor, this ranking is based on the probabilistic upper bounds on the total turnaround time for the application on a given resource. The purpose of this research is to develop the methodology behind generating these bounds.

Liu, et al. [9] extend Condor's *ClassAds* language to enable set matching, that is, to select multiple resources for a single job. Their research deals specifically with workflows, where multiple interacting components are run on separate computational resources. Their experiments considered both execution and communication costs. However, their aim is to select a set of resources that minimizes execution time; their approach does not provide insight into whether a given deadline will be met. Also, they do not consider batch queue delay. The research presented here does not include workflow applications, though this is a domain for future work.

Another approach to Grid resource scheduling is through the use of economic models

[10]. In such an approach, a computational economy framework is used for resource allocation, as well as regulating supply and demand. The computational economy is derived by charging users the value they get from their results. SPRUCE does employ a very coarse-grained economic model. SPRUCE users pay a higher price (i.e., a token) in order to secure higher priority, and they may "shop around" at the resources to which they have permission to submit urgent jobs in order to find a resource that offers the best probability of meeting their deadline. The resource providers, in turn, have a coarse ability to set their price. For instance, a resource owner can charge a higher price for a preemptive job by granting the priority to a small subset of urgent computing users. SPRUCE users that do not have permission to submit at that high urgency level are, effectively, unable to pay that price. Similarly, resource owners can choose not to offer some priority mechanisms (such as preemption). Also, resource owners may choose to charge SPRUCE users additional CPU hours for jobs that receive elevated priority. SPRUCE users will most likely be interested in paying the minimum possible to meet their deadline; however, a methodology still must be developed to determine the probability of meeting that deadline.

Nurmi et al. [11] enhance a workflow scheduler to incorporate aspects of batch queue delay [12] and application performance [13]. Their approach deals specifically with workflow applications that consist of interacting components that may execute simultaneously on distinct resources. Similar to the approach outlined in this thesis, they make use of a technique that predicts a bound on the amount of delay a job will experience in a batch queue [12]. Their results show that they are able to reduce the total turnaround time. In order to estimate the execution time, they generated a parameterized performance model based on the hardware characteristics of each resource and the application's behavior (i.e., memory usage and floating point operations). Communication costs are also included in the model. The purpose of the performance model is not to predict the exact execution time but rather to provide an estimate that can be used by the scheduler to evaluate the effectiveness of the hardware configuration for the current workflow. While containing many similarities with the work described in this thesis, there are three primary differences. First, this thesis proposes an approach that generates a bound on the total turnaround time in order to determine how likely a given configuration is to meet a deadline. In contrast, their approach seeks only to minimize the turnaround time, with no guarantees regarding the deadline. Second, they consider only communication costs between components and generate predictions using Network Weather Service probes. TCP-based Network Weather Service probes are inadequate for predicting large GridFTP file transfers, which is discussed in Chapter 4.1. Finally, their work is geared to workflow applications consisting of multiple interacting components whereas our methodology is simplified to a more traditional parallel application that executes on a single resource.

Chapter 3

Special PRiority and Urgent Computing Environment (SPRUCE)

The Grid-based SPRUCE architecture is designed to meet the following requirements:

- A "session" in which urgent computation jobs may be submitted should be clearly defined.
- The ability to initiate a session should be easily transferable to avoid a single point of failure in emergency situations.
- Users associated with a session are able to submit urgent computations to any permissible resource.
- The framework should support flexible urgent computing policy choices to be determined and implemented by Grid resource providers.

SPRUCE fulfills these requirements by using a token-based architecture. An urgent computing session begins with the activation of a token via a web portal or web service invocation. Tokens are simply 16-character strings (see Figure 3.1), which are easily transferable. Furthermore, tokens are created with three static attributes. First, each SPRUCE token is associated with a set of resources. When activated, urgent jobs will be granted high-priority access only at these resources. Second, the token is created with a lifetime, which specifies the duration of the urgent computing session. Third, each token is created with a maximum urgency level. There are three priority levels: red (critical), orange (high), and yellow (medium). Naturally, jobs with a higher urgency will displace those with a lower urgency when resources are scarce. Also, multiple levels allow the resource provider to specify multiple responses based on the urgency of a request. Once a token is created, the token-holder is able to associate a set of users with the token. Users may be added to or removed from a valid token at any time. A token is valid once it is created until its session expires. The associated users have the right to submit elevated priority jobs to any of the associated resources at the permitted urgency levels.

Figure 3.1: A SPRUCE right-of-way token.

One of the defining design features of SPRUCE is that computational resource policies are created and implemented by the resource owners. That is, SPRUCE does not dictate how a resource must respond to an urgent computation request. For instance, two resources could have the policies depicted in Table 3.1. In this example, Resource 1 has different responses for each urgency level and, as the urgency increases, so does the response. Resource 2, in comparison, effectively ignores "medium" priority jobs (i.e., treats them as normal, non-SPRUCE jobs) and handles "high" and "critical" jobs in a similar fashion. This flexibility allows resource owners to retain ultimate control over their resources and will lead to an easier adoption of SPRUCE by resource owners.

Table 3.1: Hypothetical resource policies for urgent computing requests. Policies are decided locally and not dictated by SPRUCE.

Urgency	Resource 1	Resource 2
Medium	Elevated queue priority	Normal
High	Next-To-Run	Next-To-Run
Critical	Preemption	Next-To-Run

Currently, the scientists must determine the urgency level of their request based on the perceived importance of their computation. However, it is important that SPRUCE users adhere to the policies in place at each resource and use good judgment. All urgent computing job submissions are logged, and misuse is handled by the appropriate system administrators. Such policy issues are outside the scope of this thesis.

3.1 Warm Standby

In order for emergency applications to be ready for an urgent computation, the application must be ready for immediate use (i.e., there is no time to test, debug, or tune the application). Thus, the code must be "frozen" in a ready-to-run state. In terms of SPRUCE, such an application is said to be in "warm standby." In a Grid environment, many potential large-scale computational resources may be available. Because there is no time to port an application to a new system in an urgent situation, part of the warm standby process includes selecting a small set of resources that are well suited for the given application. Furthermore, the warm standby process includes periodic tests of the application on the selected resources. These tests will ensure that there have been no underlying changes in the Grid infrastructure (e.g., changes to the computational resource environment and GridFTP servers continue to function properly). In addition, periodic testing will also enable performance monitoring of the application on the various computational resources, which will be useful for generating bounds on execution delay as well as creating a validation history.

Chapter 4

Advisor: Deadline-Based Grid Resource Selection

The purpose of this master's degree research is to develop and evaluate a set of methodologies and heuristics that can aid a user in resource selection for urgent computing. This is primarily achieved by generating a probabilistic upper bound on the total turnaround time for the urgent computation on a particular resource. The total turnaround time, as depicted in Figure 4.1, consists of the file staging delay (both input and output), the resource allocation delay (i.e., batch queue delay), and the execution delay.

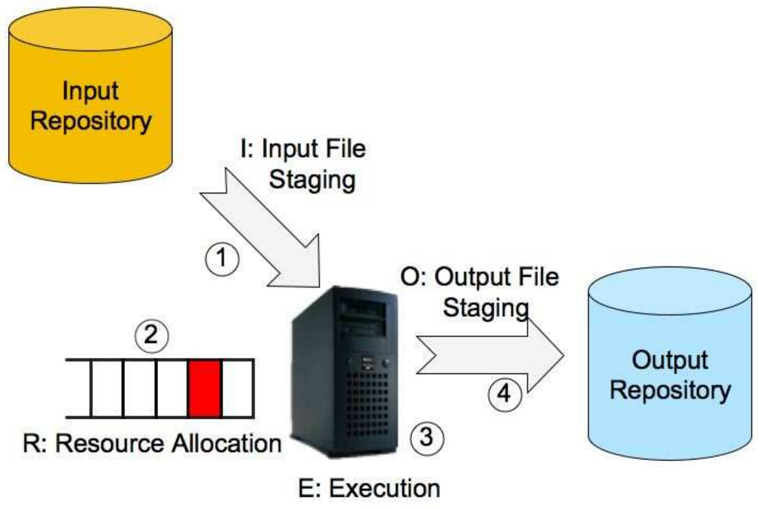

Figure 4.1: The four phases of the total turnaround time for an urgent computation. First, any necessary input files are staged to the resource (1). Then, the computation is submitted to the batch scheduler (2). Third, the job executes on the resource (3). Finally, any output file staging is completed (4).

An urgent computation may have many *configurations*. A configuration consists of a single specific instance of an urgent computation. For example, consider an application that has three warm standby resources. On each resource it has amassed performance data for runs on 64 and 128 nodes. The application requires one input file that is available from four different repositories. The application may be submitted at all SPRUCE urgencies (i.e.,"medium," "high," and "critical") and normal priority (i.e., no SPRUCE) at each resource where each urgency results in a distinct policy. Thus, there are 96 different configurations (3 resources * 2 node specifications * 4 input repositories * 4 policy choices = 96). The user is interested in knowing which configuration provides the greatest probability of meeting a given deadline.

For a given configuration, one can predict an upper quantile on the total turnaround time, which serves as a probabilistic upper bound. For instance, if the 0.95 quantile for the delay is 100,000 seconds, then there is a 95% chance that the delay will be less than 100,000 seconds. Each of the individual phases of the total turnaround time (see Figure 4.1) may be bounded individually: (i) input file staging delay (quantile I_Q corresponds to an upper bound I_B), (ii) resource allocation delay (e.g., queue delay) (R_Q, R_B), (iii) execution delay (E_Q, E_B) and (iv) output file staging delay (O_Q, O_B). In the simple case where each of these phases is independent (i.e., no overlap), a bound on the total turnaround time can be computed as follows:

An upper I_Q x R_Q x E_Q x O_Q quantile corresponding to a bound of
$$I_B + R_B + E_B + O_B.$$

This composite quantile is conservative in that the composite quantile is *at least* the product of the individual quantiles. In reality, this value represents the probability that all four upper bounds are satisfied individually. For example, if each of the four individual phases is bounded by an upper 0.95 quantile, then the composite quantile is the upper 0.815 quantile. This corresponds to a probabilistic upper bound that there is an 81.5% chance all four individual phase upper bounds are satisfied. Clearly, if each individual bound is exceeded, then the sum of the individual delays will exceed the composite upper bound. However, this composite quantile does not include the situations where at least one of the individual bounds is satisfied as well as the composite bound. This occurs when the overprediction of the satisfied bound compensates for the underprediction of the individual bound or bounds that are exceeded. In the context of urgent computing, this conservativeness is acceptable, as it is better to err on the conservative side in order to reduce the chances that the results are produced after the deadline.

In the following three subsections, the methodology for predicting the individual phase quantiles is presented. For the most part, these calculations use pre-existing technologies. The novel contributions and uses of this research will be highlighted.

4.1 Input and Output File Staging Bounds Prediction (I_Q, I_B and O_Q, O_B)

The underlying methodology for bounding the input and output file staging delays (phases 1 and 4 in Figure 4.1) is the same. In the case of multiple input or output files that originate from a single source or are transferred to a single destination, it is preferred to transfer the input or output data as a single bundled transfer. This procedure will avoid lowering the overall quantile that occurs when the quantiles are combined to generate a composite upper bound.

The predicted upper bound for the output file staging delay suffers from an inherent obstacle, namely, that the predictions are based off the current network bandwidth but the actual file transfers will not occur until some later point in time (i.e., after the conclusion of the input file staging, resource allocation and execution phases). The greater the span of time between the prediction and actual transfer, the greater the probability that the bandwidth behavior may have changed. Part of this research examines how the performance of these predictions fare in a case study application (see Chapter 5) where the output file staging occurs 2–15 hours after the predictions are made.

The Network Weather Service (NWS) provides the necessary functionality to periodically measure the bandwidth between a source and destination and make predictions on expected bandwidth [14]. Furthermore, a probabilistic upper bound can be created for some measurement streams by using the mean square error (MSE) as a sample variance of a normal distribution and then calculating the upper confidence interval. For example, one can calculate the upper 95% confidence interval as $forecast + 1.64 * \sqrt{MSE}$. However, complications arose while trying to predict the bandwidth achieved for GridFTP transfers using the TCP-based NWS probes. In many cases, particularly involving sources and destinations that were part of the TeraGrid [15] that exhibited high bandwidth rates, the probes were unable to match the bandwidth behavior achieved by the GridFTP transfers. For an example of this problem, see Figure 4.2. Here, the transfers exhibit much more variability and a higher peak bandwidth. The transfers also exhibit more of a bimodal appearance. Moreover, the probes and transfers both appeared to be traveling the same path from source to destination and modest attempts at scaling up the probe size were not helpful. In another experiment, the size of the file used in the GridFTP transfers was modified to match the size of the probes. In Figure 4.3, the results of one such experiment are shown. As before, the transfers exhibit a bimodal behavior and a higher peak bandwidth. One tool that was useful in comparing the bandwidth series was *ts_comp* [16]. This tool uses techniques that remove differences in shift and scale while comparing one time series with another. In many cases, however, the tool was unable to report a similarity matching between a probe series and the corresponding GridFTP transfer series.

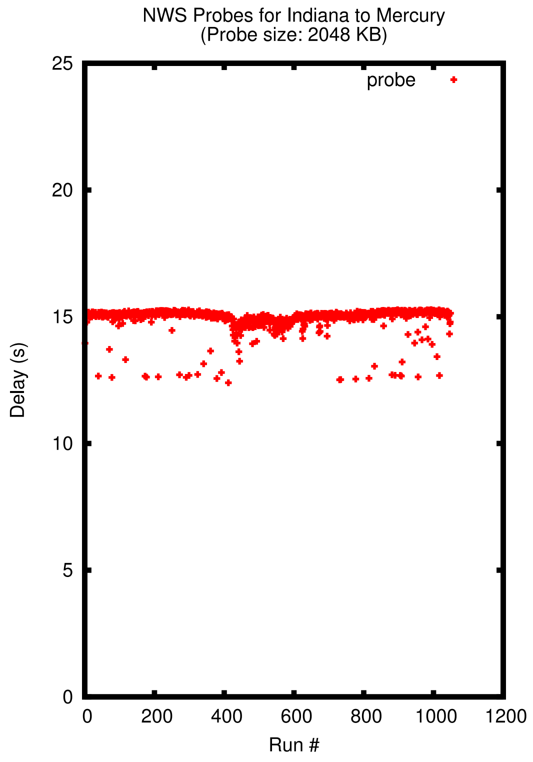

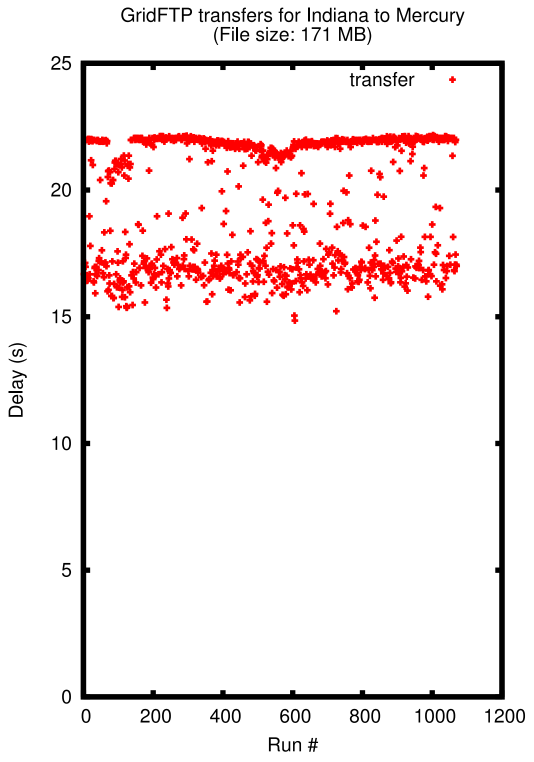

Figure 4.2: On the left is a plot of the bandwidth achieved by 1,049 2 MB TCP-based probes that are sent every 15 minutes between the Indiana input source and Mercury. On the right are the corresponding transfers of a 171 MB file that is transferred via GridFTP every 15 minutes.

The above data clearly indicates that the small TCP-based probes used by NWS are unable to match the behavior of GridFTP transfers. As a result, a GridFTP probe framework was implemented that periodically measures the bandwidth between the source and destinations by transferring probes via GridFTP. These probes were individually tuned for each source-destination pair until the probe bandwidth and transfer bandwidth were similar. The GridFTP framework produced results that more closely matched the behavior of the actual GridFTP transfers. An actual NWS

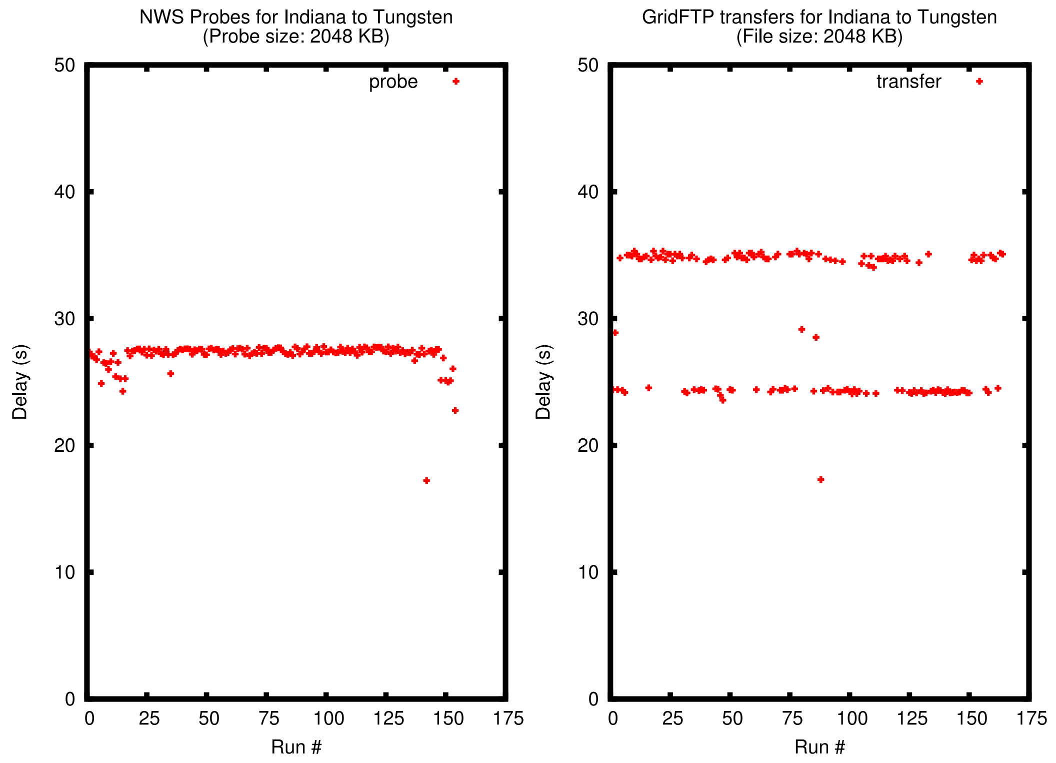

Figure 4.3: On the left is a plot of the bandwidth achieved by 154 2 MB TCP-based probes that are sent every 15 minutes between the Indiana input source and Tungsten. On the right are the corresponding transfers of a 2 MB file that is transferred via GridFTP every 15 minutes between the source and destination.

installation is still used to track each series and generate the necessary probabilistic bounds based on those probes.

4.2 Resource Allocation Bounds Prediction (R_Q, R_B)

The resource allocation delay (phase 2 of Figure 4.1) represents the amount of delay from when a job is submitted to a resource until it begins execution. One of the primary methods that SPRUCE uses for urgent computing is reducing the batch queue delay through elevating the priority of urgent computations. However, the amount of queue delay an urgent computation will experience depends not only upon the resource load, but the local policy that each resource implements for the given urgency level. This policy details how urgent requests are handled. Currently, two policies have been implemented, other than the normal (i.e., no SPRUCE) priority:

1. Next-to-run – The job is designated as the next job to run.
2. Preemption – If necessary, jobs that are currently executing are killed to free up the necessary resources for the preemptive job.

In order to generate the probabilistic bounds for the normal priority resource allocation delay, the existing Queue Bounds Estimation from Time Series (QBETS) [17] technology is used. This service is already included in the TeraGrid portal. At the heart of the QBETS methodology is a technique the authors call the Binomial Method Batch Predictor (BMBP) [12]. For computations that are submitted at a normal priority, QBETS can be queried for a desired upper quantile. Currently, the tool supports the upper 0.95, 0.75, and 0.50 quantiles for a given resource and queue.

For the next-to-run priority, the authors of QBETS have modified their tool in order to generate bounds for next-to-run jobs. In the modified tool, a Monte Carlo simulation of next-to-run batch queue delays is conducted based on previously observed job history. This simulation produces a distribution of next-to-run delays for a number of different job sizes. From these distributions, the tool predicts bounds on the next-to-run delay for a job using the same internal software infrastructure as the original QBETS. Part of the purpose of this research is to validate this methodology for the next-to-run priority. Also, it is the first example of using this bounds generator in the context of resource selection.

For the preemption policy choice, the authors of QBETS have extracted the BMBP methodology that is at the heart of QBETS to create a tool that can be applied to an unknown distribution rather than a time series. This tool is then used to predict bounds on the preemption delay based on previously observed preemption delays for similarly sized jobs. This research is the first to attempt to use this methodology in such a manner. The methodology appears to be a good fit because it is nonparametric and general.

The probabilistic bounds generated for the preemption policy involve a number of assumptions. For example, it is assumed that there are enough nodes available to preempt. In two cases, this assumption may not hold. First, there may not be enough responsive nodes available to preempt; for example, if a resource has 64 nodes but 10 nodes are down, it will not be able to allocate a preemptive job requesting more than 54 nodes. Second, depending on the policy, preemptive jobs may not be able to preempt other preemptive jobs (such is the case at the UC/ANL IA-64 TeraGrid resource). In this case, a preemptive job will wait in the queue until there are enough nodes freed up by the completion of earlier preemptive jobs. In such a scenario it is assumed that the bounds predicted will be incorrect. Also, the preemptive bounds generated by this method assume that a resource is completely used. In other words, the history used by the methodology only includes samples of when all the requested nodes had to be preempted. In practice, some of the requested nodes may already be free, resulting in a shorter preemption delay because fewer nodes are being preempted.

Several situations may arise in which the above methodologies will perform poorly. For example, consider the case where a resource is idle and the requested nodes are immediately available. In this situation, a job could be submitted with no SPRUCE urgency and begin executing almost immediately. However, the bounds generated for the various policies would most likely be excruciatingly conservative despite the fact that this scenario is clear from the current state of the resource. This situation occurs because the above methodologies generate resource allocation bounds based on past job history and not on the current queue state. As another example, consider the situation where it is clear from the queue state that there may be a queue delay that exceeds the predicted upper bound. Such an instance may occur for a normal priority job when a massive job is submitted that requests most of the nodes begins executing before the urgent computation. For a SPRUCE job, a similar situation arises when other SPRUCE jobs of the same or higher priority are submitted prior to the job in question. These situations are a direct result of predictions that are based entirely off of historical data. While the historical data may provide correct predictions from a mathematical standpoint, there may be cases where simple inspection of the current state may provide additional insight. For resources using the Globus toolkit, the current state of the resource may be available via the Monitoring and Discovery Services framework (MDS) [18]. This framework allows for the current state of participating resources to be discovered via a web service call. Thus, by reporting back both the probabilistic bound and the current state of the resource, a user can ascertain whether such situations exist.

4.3 Execution Bounds Prediction

Similar to preemption batch queue bound predictions, the modified BMBP tool is again used to generate probabilistic upper bounds on the execution delay (phase 3 in Figure 4.1). Again, the present research is the first to use this methodology to predict an upper bound on execution delay. This approach exploits the fact that the warm standby mechanism will be creating a log of periodic executions of the application on typical input sizes in order to validate that the application is ready for urgent use.

4.4 Improving the Composite Quantile and Bound

As mentioned, the composite quantile is conservative in that it represents the probability that the delay for each of the individual phases (i.e., file staging, resource allocation, and execution) is satisfied. Even when targeting high quantiles for the individual phases, the composite quantile quickly decreases (e.g., targeting the 0.95 quantiles for input file staging, resource allocation, execution and output file staging results in the composite 0.815 quantile). However, the composite quantile can be increased, either through overlapping phases of the urgent computation or through speculative execution. Each of these approaches is briefly discussed below.

4.4.1 Overlapping Phases of the Urgent Computation

In the above formulation of the composite upper bound, the clause of independence requires that the four phases occur one at a time (e.g., no overlap). By requiring phase independence, however, one ignores a relatively straightforward opportunity to both reduce the composite bound and increase the corresponding quantile. The most obvious opportunity for overlap is by staging the input files while the job is waiting in the batch queue (see Figure 4.4). Clearly, the application must be able to handle the situation in which it begins execution before the input data arrives. A simple solution (though potentially wasteful in terms of unnecessary cycles) is to have the application "spin" until the input is available. In this situation, any time that the application spends in the queue while data is being transferred is an actual decrease in the overall delay of the total turnaround time. However, the primary benefit is in the calculation of the bound. Consider the following example. For a given urgent application, the input files have a probability of 0.90 of being transferred in 10 minutes, a probability of 0.95 of being transferred in 20 minutes, and a probability of 0.99 of being transferred in 30 minutes. Similarly, the job has a probability of 0.75 of beginning execution in 10 minutes, a probability of 0.85 of starting execution in 20 minutes, and a probability of 0.95 of starting execution in 30 minutes. In the serial case, one could generate a composite 0.90 quantile by combining the individual 0.95 quantiles; in this case, that is an upper 0.90 quantile of 50 minutes. But, in the overlapping case, if the target job start time is the 0.95 quantile of 30 minutes, there clearly is a probability of 99% that the files will be done transferring in 30 minutes. Thus, the composite upper bound in this case is actually the 0.94 quantile of 30 minutes. In comparison to the serial case, we decreased the bound (30 minutes rather than 50 minutes) while increasing the quantile (0.94 versus 0.90). In general, for two phases that overlap completely (i.e., start at the same time), the composite upper quantile is the product of the two individual quantiles. and the corresponding bound is the maximum of the two individual bounds.

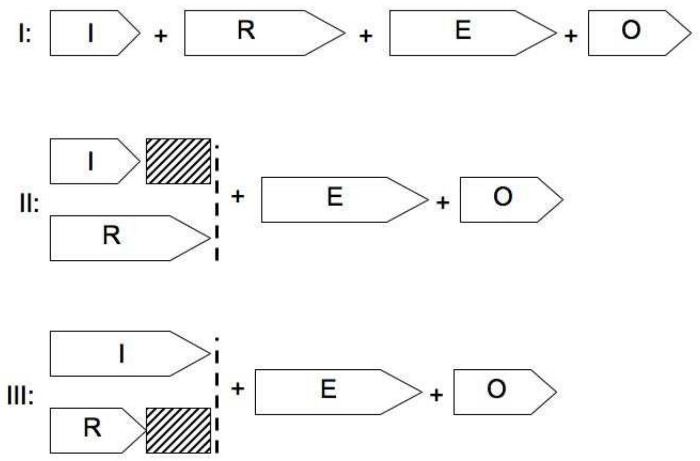

Figure 4.4: Timeline for the serial and overlapping phases of an urgent computation. In I, the phases are serial. In II and III, the input and resource allocation phases are overlapped. In II, the input phase completes prior to completion of the resource allocation phase. In III, the resource allocation phase completes prior to the end of the input file staging phase. In this case, the portion of time from when the resource allocation phase ends until the input file staging phase ends represents wasted cycles, where the computation "spins" until the input is ready.

4.4.2 Speculative Execution of Independent Configurations

In Chapter 2, Schopf suggests speculative execution as a means to increase reliability. In terms of urgent computing, submitting multiple, independent configurations simultaneously can improve the probability of meeting the deadline for at least one of the configurations. Consider the case where a user simultaneously initiates two independent configurations of an urgent computation. If the first configuration has a probability of $Pr(config_1)$ of meeting the deadline and the second configuration has a probability of $Pr(config_2)$ of meeting the deadline, the probability that at least one of the configurations meets the deadline is $Pr(config_1) + Pr(config_2) - Pr(config_1)Pr(config_2)$. This formulation requires that $config_1$ and $config_2$ be independent events. Specifically, it requires that neither configuration utilizes the same input repository, computational resource, or output repository.

4.5 Optimizing the Probabilistic Bound for a Configuration

The above methodology describes how to generate a conservative composite upper bound on the total turnaround time for an urgent computation configuration. The composite quantile consists of the product of the individual phase quantiles. Clearly, by computing a different quantile for an individual phase, the composite quantile and bound will change as well. Thus, to determine the "optimal" probabilistic upper bound, the Advisor needs to find the combination of individual quantiles that generates the highest quantile that corresponds to a bound less than the deadline. It is more advantageous to maximize the probability rather than minimize the bound because the urgent-computing user is most interested in the probability of meeting the deadline. For example, if the deadline is in six hours, it is more useful to know that there is a 75% chance of the urgent computation completing in five and a half hours rather than a 20% chance of finishing in less than two hours. The current methodology implemented by the Advisor is to query a small set of points for each phase and then consider all possible combinations. The highest composite quantile with a bound less than the deadline is then associated with the given configuration. If no such quantile exists, then that configuration may be ignored as the calculated probability of meeting the deadline is small. Then, the remaining configurations are presented to the user with their associated probabilities.

4.6 Limitations of the Composite Bounds

The composite upper bounds generated for this research have a number of limitations. First, an urgent computation is assumed to consist of a traditional parallel code rather than a workflow comprising of multiple interacting components that execute simultaneously on distinct resources. Second, the probabilistic bounds that are generated correspond to the probability of a single instance of the urgent computation. These bounds are not valid for multiple instances of the configuration. For example, if a user simultaneously submits 100 instances of a single urgent computation configuration, the bound is not valid for all of the instances. In such a scenario, the inherent correlation is not addressed by the predicted bounds. This situation is different from the speculative execution scenario in which independent configurations are submitted simultaneously; in the latter case, there is little correlation.

Chapter 5

Case Study

In order to evaluate the methodologies just described for generating composite upper bounds on the total turnaround time, experiments were conducted using FLASH [19] as a sample scientific simulation. FLASH is a modular, multiphysics, adaptive-mesh astrophysics code developed at the University of Chicago Astrophysics Department. It is used to study a variety of astrophysical phenomena and has scaled on some of the largest high-performance computing systems in the world. The “cellular” problem used for this research involves the material flows during nuclear burning. The case study application executes 1,000 time steps using eight levels of mesh refinement. While FLASH may not be an ideal urgent computing application, it was selected because it is an example of a well-known scientific computing code with a high level of local expertise (i.e., University of Chicago).

The FLASH code was ported to the three TeraGrid resources listed in Table 5.1, which served as the set of warm-standby resources. In order to seed the execution bounds predictor for each resource, 100 trials of the application were completed on each resource, and their execution delays (as reported by the various batch queue logs) were recorded.

Table 5.1: The three warm standby resources for the case study application.

Name	CPU	Nodes	CPUs
UC/ANL IA-64	Itanium 2 Madison (1.3/1.5 GHz)	62	124
Mercury (fastcpu)	Itanium 2 (1.5 GHz)	631	1262
Tungsten	Intel Xeon (3.5 GHz)	1280	2560

While the FLASH simulation does not require any file staging, this requirement was artificially added into the case study in order to create a full urgent computation that consists of all four phases of delay (i.e., input file staging, batch queue, execution and output file staging). The data movement requirements were loosely modeled after the requirements of a Linked Environments for Atmospheric Discovery (LEAD) [20] workflow. LEAD is one of the first users of the SPRUCE framework, and in 2007 the team worked with SPRUCE to perform real-time, on-demand, dynamically adaptive forecasts [21]. For the case study, a 3.9 GB input file is required prior to execution. The input data is available via GridFTP from two locations, the University of Indiana and the University Corporation for Atmospheric Research (UCAR). The (artificial) output data is similarly sized and must be transferred to a server at the University of Indiana.

The case study consists of the six experiments outlined in Table 5.2. The remainder of this chapter discusses each experiment and its results.

5.1 Experiment 1: GridFTP

The purpose of the first experiment was to validate the upper bounds for the input file staging phase for the UCAR input repository. The configurations that consisted of the UCAR input repository were omitted from later experiments in order to reduce the overall number of complete trials of the case study that were completed. If the bounds for the input file staging phase are correct, as well as the bounds for the resource allocation, execution, and output file staging phases of later experiments, one can infer that the total turnaround time bounds most likely would have been correct as well. The UCAR host resides outside the TeraGrid network, and the transfers were significantly slower than those originating from the alternative input repository at Indiana. In this experiment, the upper 0.95 quantile was predicted for

Table 5.2: Brief description and purpose of each of the experiments in the case study.

#	Name	Description	Purpose
1	GridFTP	Test predicted bounds for GridFTP transfers.	Validate the methodology for bounding GridFTP transfers from UCAR input source.
2	Normal	Test configurations utilizing normal (i.e., no SPRUCE) priority.	Evaluate composite methodology performance on normal priority.
3	Next-to-run	Test configurations utilizing next-to-run priority.	Evaluate composite methodology performance on next-to-run priority. Further validate next-to-run bounds predictor.
4	Preemption	Test configurations utilizing preemption priority.	Evaluate composite methodology performance on preemption priority. Validate preemption bounds predictor.
5	Overlap	Test configuration with overlapping phases.	Evaluate gains from overlapping input and queue phases.
6	Advisor	Test approximate optimization of quantile methodology.	Demonstrate algorithm to optimize composite quantile and discuss results.

the transfer of a GridFTP file from the UCAR host to each of the three case study resources (see Table 5.1). This procedure was repeated at least 100 times in order to track the success rate. The results of these experiments, summarized in Table 5.3, indicate that the methodology is doing a reasonable job in generating an accurate and relatively tight upper bound.

Table 5.3: Results from experiments generating an upper 0.95 quantile bound on the delay achieved in a large GridFTP transfer from the UCAR input source to one of the case study resources. The transferred file was 3.9 GB.

Destination	# of Trials	Percent < Bound	Percent Overprediction
UC/ANL IA-64	112	100	8.5
Mercury	113	91.2	4.90
Tungsten	364	95.9	25.89

5.2 Experiment 2: Normal Priority

The purpose of the second experiment was to validate the correctness of the bound methodology for the total turnaround time for configurations using normal priority. For this experiment, both the individual and composite bounds for the normal priority (i.e., no SPRUCE) configurations on all three resources were studied. Because the UC/ANL resource is much smaller, the application runs on 16 nodes with 2 processors per node, whereas 32 nodes with 2 processors per node are requested for Tungsten and Mercury. In these configurations, the Indiana source was used for input file staging. For each of the individual phase bounds, the upper 0.95 quantile was predicted. Thus, the resulting composite bound represents the upper 0.815 quantile (i.e., $0.95^4 = 0.815$).

The composite upper bounds and actual delays from the three configurations are depicted in Figure 5.1. For the UC/ANL IA-64 resource, the predicted bounds

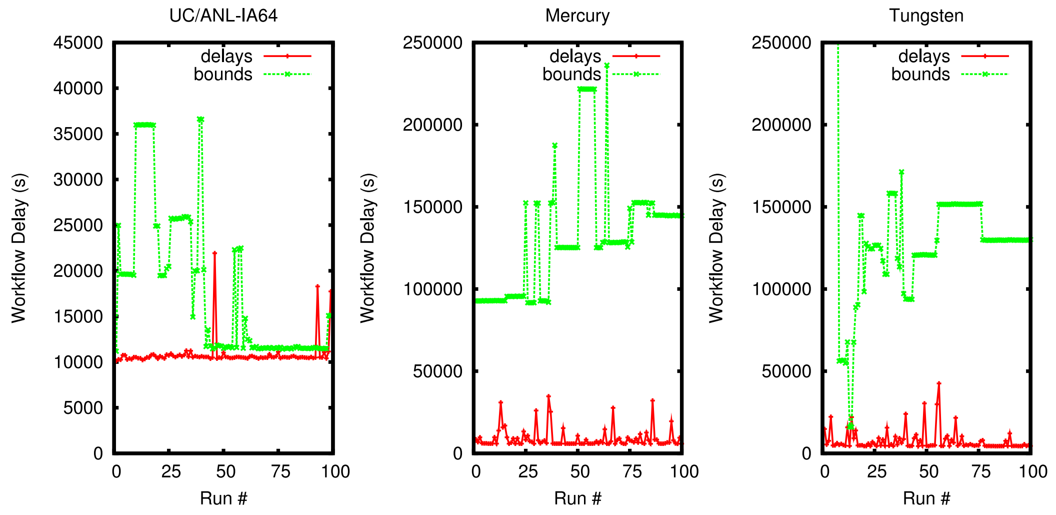

Figure 5.1: Predicted upper 0.815 quantile versus the actual the delay achieved by the configurations using the Indiana input source and normal priority for the UC/ANL IA-64, Mercury and Tungsten resources. Note the different scales between the UC/ANL resource and Mercury/Tungsten.

experience a significant drop midway through the experiment and closely follow the actual delays (see Figure 5.1). This is caused by the underutilization of the resource. In this experiment, 72 of the 99 completed runs experience a queue delay of one second or less. In addition, much of the time the only job queued on the resource was the case study job. These factors combined to create a bias in the predicted bounds because the stream of case study jobs was submitted during a period of low activity on the resource. Hence, a change point in the batch queue delay time series was detected by QBETS, and the predicted delays were drastically reduced. However, the data still shows that the predicted upper bound is serving its purpose in that the target probability of overall success is being met.

The results of the individual phase upper bounds as well as the overall bounds are summarized in Table 5.4, and the overprediction percentage for each phase is listed in Table 5.5. The success rate of the input file staging bounds for Tungsten is only

88%. However, several factors contributed to the low success rate. First, during the experiments, the dedicated Tungsten GridFTP server was experiencing problems that would not allow incoming connections. Hence, few probes were completed, thereby hindering the bounds predictions. After 15 runs, the experiments were shifted to use the login nodes as the GridFTP server. While this strategy eliminated the connection problem, it introduced another: the performance was a lot more variable as the server was no longer dedicated solely to handling GridFTP traffic. This variability was evident in the both the probes and actual transfers.

Table 5.4: Percentage of measurements that were less than the predicted upper bound for the configurations using the Indiana input source and normal priority. For the individual phases (i.e., input, queue, execution, and output), the target quantile was 0.95; for the overall bound, the quantile was 0.815.

Resource	# of Trials	Input	Queue	Execution	Output	Overall
UC/ANL IA-64	99	100%	97%	100%	83%	97%
Mercury	100	99%	99%	93%	86%	100%
Tungsten	100	88%	99%	96%	77%	99%

Table 5.5: Percent overprediction for each phase of the configurations using the Indiana input source and normal priority.

Resource	Input	Queue	Execution	Output	Overall
UC/ANL IA-64	7.98%	2,379.09%	7.01%	21.89%	64.95%
Mercury	10.19%	4,468.23%	3.78%	5.29%	1,417.26%
Tungsten	10.57%	4,811.20%	13.03%	-4.63%	1,842.43%

The upper bounds for the queue phase all exceed their target 95% hit rate. However, the overprediction percentage clearly shows that the bounds are not very accurate. This problem arises from the variability in batch queue delays. For example, as mentioned above, most of the time (72 out of 99 trials) the batch queue delay in the UC/ANL IA-64 configuration was one second or less. However, three queue delays were more than 6,900 seconds, including one that lasted over 10,800 seconds. In the case of Mercury and Tungsten, the overprediction rate is even worse, as they both exceed 4,000%.

The execution bounds for all three phases do particularly well in terms of correctness and tightness. Both the UC/ANL and Tungsten resources exceed the target 95% success probability, with Mercury performing just below at 93%. The overprediction rates are also reasonable, at less than 14%. These results indicate that the BMBP tool is performing well, thus supporting its use as the execution delay bounds predictor. Again, one of the reasons it was selected was its general nature. This is highlighted by the UC/ANL resource, which consists of processors of two different clock speeds (1.5 and 1.7 GHz). As a result, the execution delay is bimodal, yet these results show not only a 100% success rate but also a very tight bound.

The results for the output phase are also promising. First, this phase possesses the inherent challenge that the bounds predictions are made for the bandwidth at a given point in time, but the transfer is not initiated until some later point. Even if there is no significant queue delay, the predictions are still for some point two to three hours in the future for this experiment. And, in the worse case, the output phase did not begin until more than 12 hours after the predictions were made. For the UC/ANL IA-64 resource, all 17 misses (as seen in Table 5.4) occurred in a span of 18 trials. During this time, there was a problem with the probe framework and practically no probes were getting through. The result was that the bounds predictions were not adjusting to the current bandwidth. Once the probes began getting through, the predicted bounds were not exceeded in any of the remaining 70 trials. For Mercury, two of the output transfers actually failed because one of the GridFTP servers did not allow a connection. The remaining 12 misses were often the result of making predictions for transfers occurring in the future. This was evident in the data, where often after one of the misses, the prediction for the output bound of the subsequent trial would see a large increase. This corresponds to the probes detecting a change in the network bandwidth and adjusting the bounds—an adjustment that would occur during the trial in question but not be reflected in the predicted upper bound. In the case of Tungsten, the problems with the GridFTP servers were previously discussed. Nine of the misses occurred while using the misbehaving dedicated server, which experienced very few probes getting through. The remainder of the misses occurred while using the more variable login node as the GridFTP server.

The overall bounds perform well, in terms of correctness. Each of the resources experience a success rate greater than 96% while the conservative target rate is only 81.5%. The reason for the success was due primarily to the conservative nature of the batch queue bounds. Often, the predicted batch queue bound was nearly as large as the actual delay of the total turnaround time. For these experiments, the overprediction of the batch queue phase always accounted for the misses in other phases. The average delay for each configuration along with the average predicted bounds are presented in Table 5.6. The conservative nature of the bounds is particularly evident for Mercury and Tungsten, where the bounds are more than an order of magnitude larger than the actual delay.

Table 5.6: Average delay and bound (in seconds) for the total turnaround time of the configurations using the Indiana input source and a normal priority.

Resource	Average Delay	Average Bound
UC/ANL IA-64	10,833	17,869
Mercury	8,696	131,951
Tungsten	7,631	148, 233

The results of this experiment indicate that the composite bounds are correct but not very accurate. The primary reason for the inaccuracy is the overprediction of the batch queue delay bounds. This is a result of the inherent variability in batch queue delay for highly used computational resources. However, this inaccuracy was also evident in the relatively underused UC/ANL resource. This overprediction is also an implicit argument for SPRUCE, which aims to reduce batch queue delay through elevated priority. As a result, the bounds for SPRUCE jobs should be lower and tighter than the bounds generated for normal jobs.

5.3 Experiment 3: Next-To-Run Priority

The purpose of the third experiment was to further validate the next-to-run bounds predictor and demonstrate the utility of the composite bounds for a SPRUCE urgent computation. The next-to-run experiment consisted of using the Indiana input source, UC/ANL IA-64 resource (16 nodes with 2 processors per node), and an urgency level of "high." At this point, there was an execution history of roughly 200 trials, 100 to seed the bounds predictor and 100 trials from the normal configuration experiment. Because the execution bounds in the previous experiment performed well, the execution delay for this experiment was emulated by randomly sampling the execution history. The aim was to avoid the needless wasting of CPU cycles by continually running the case study application. In order to generate valid queue delays, however, a dummy job (e.g., *hello world*) was submitted to the batch scheduler requesting the same number of nodes and wall clock time as before. Once the dummy job finished execution, the execution delay was sampled and the case study urgent computation slept for the appropriate time. As was the case in the normal configuration experiments, the 0.95 quantile was predicted for the four individual phases, with the resulting composite 0.815 quantile for the total turnaround time.

The predicted bounds plotted against the actual delay are shown in Figure 5.2. Here, the projected bounds are much tighter than in the previous experiments using normal priority. In all, 98 trials of this configuration were completed. The results of the predicted bounds are summarized in Table 5.7, and the overprediction percentage for each phase is listed in Table 5.8.

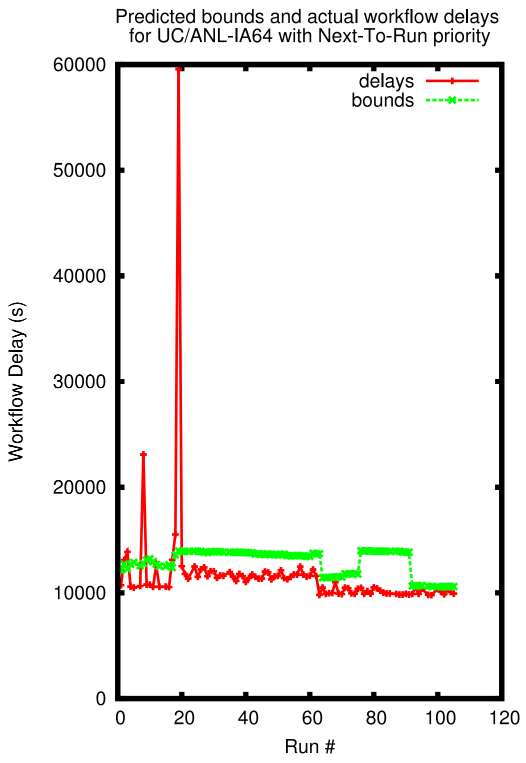

Figure 5.2: Predicted upper 0.815 quantile versus the actual delay achieved by the configuration using the Indiana input source and next-to-run priority for the UC/ANL IA-64 resource.

Table 5.7: Percentage of measurements less than the predicted upper bound for the configuration using the Indiana input source, next-to-run priority, and UC/ANL resource. For the individual phases (i.e., input, queue, execution, and output), the target quantile was 0.95; for the overall bound, the quantile was 0.815.

Resource	# of Trials	Input	Queue	Execution	Output	Overall
UC/ANL IA-64	98	100%	92%	91%	92%	94%

Table 5.8: Percent overprediction for each phase of the configuration using the Indiana input source, next-to-run priority, and UC/ANL resource.

Resource	Input	Queue	Execution	Output	Overall
UC/ANL IA-64	8.04%	46.37%	4.54%	41.47%	11.27%

With the next-to-run priority, the success rate of the upper bound for the queue phase is just under 92%. However, all of the misses occurred at the beginning of the experiment (in the first 20 trials). During this time, there was a burst of activity on the resource, including the submission of 25 8-hour, 8-node jobs. The result was that the next-to-run jobs would actually have a nontrivial batch queue delay. However, this delay was smaller than if the case study job had been submitted as a normal job. In that case, that job would have most likely waited until nearly all of the 8-node jobs had finished. There was also a single 24-hour job submitted that requested enough nodes such that the next-to-run job could not begin. In the plot, this corresponds to the single large spike of the actual delay which occurred when the job waited in the queue for over 13 hours. Noteworthy, however, is the fact that the overprediction percentage has dropped to roughly 46%, a substantial improvement on the overprediction rate that occurred for the normal configuration on the same resource.

For the total turnaround time bounds, a success rate of nearly 94% was achieved with a significantly smaller overprediction rate than achieved in the normal priority experiments. These results clearly indicate that the composite bounds are not only correct but also more accurate. Moreover, the results offer further validation of the next-to-run bounds predictor, which is producing correct bounds that are significantly tighter than the normal priority bounds. Consequently, the composite bounds are also much tighter, which is evidenced by the fact that the average trial had a delay of 11,562 seconds and the average composite bound was 12,966 seconds.

5.4 Experiment 4: Preemption Priority

The purpose of the preemption experiment was to validate the bounds prediction methodology for the preemption policy. This experiment consisted of the configuration using the Indiana input source, UC/ANL IA-64 resource (16 nodes, with 2 processors per node) and urgency level of "critical." As was the case in the normal configuration experiments, the 0.95 quantile was predicted for the four individual phases, with the resulting composite 0.815 quantile for the total turnaround time. The preemption bounds were generated from a history of 100 preemption trials that were used to seed the bounds generator. In order to avoid the clear impact on jobs outside of the case study, both the 100 preemption seed trials and the trials for this experiment were conducted as follows. First, a job was submitted that requested the necessary number of nodes (i.e., 16). Then, a preemptive job was submitted to the same set of nodes. This avoided the unnecessary killing of outside jobs. For this experiment, the dummy job was submitted and allowed to begin execution prior to the bounds predictions and initiation of the trial. As in the next-to-run case, the execution delay for the preemptive job was emulated from the execution history.

The plot of the actual delay versus the predicted bounds is depicted in Figure 5.3. In all, 109 trials of this experiment were conducted. Similar to the next-to-run experiments, the upper bound is relatively tight. In contrast to the next-to-run experiment, there are no large spikes in the actual delay that exceed the predicted bounds by a large margin. This is a result of the fact the preemption policy eliminates some of the variability that can occur in batch queue delay. Even with the next-to-run policy, there were instances where the resource was fully used and the job was queued for a significant amount of time. It is important to note that with both the next-to-run and preemption policies, large batch queue delays can occur if other SPRUCE jobs are currently executing or queued that are of equal or greater urgency. This situation was not addressed in this case study, though the Advisor provides a summary of the current queue state to the user that includes the number of SPRUCE jobs currently running and queued on the resource.

The results of the individual and composite bounds are depicted in Table 5.9, and

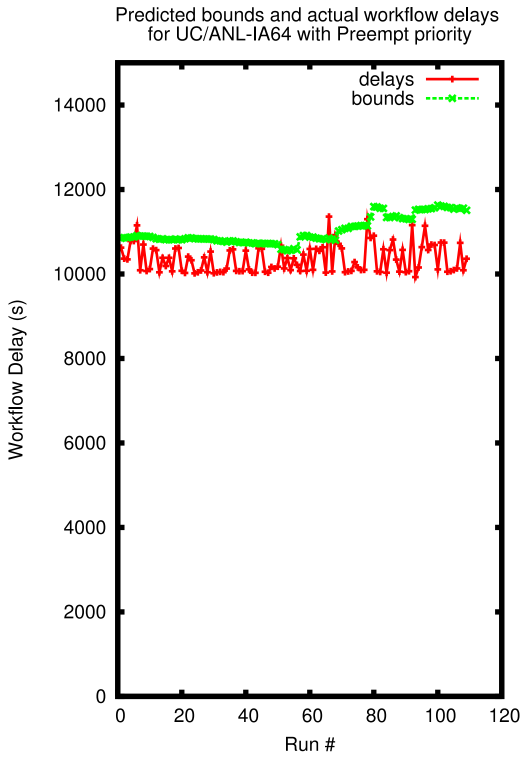

Figure 5.3: Predicted upper 0.815 quantile versus the actual delay in using the Indiana input source, preemption priority, and the UC/ANL IA-64 resource. A total of 109 trials were conducted.

the overprediction percentages are summarized in Table 5.10. Of interest are the batch queue bounds, which achieved a 94% success rate. The overprediction rate for the preemption bounds was 75%. This was due to the variability seen in the preemption delays throughout the experiments. Typically, the preemption delay for 16 nodes was around 170 to 300 seconds. During these experiments, however, there were a number of times where the delay was significantly longer, including a delay of over 1,300 seconds. Several problems with the resource (e.g., node configuration errors) also cropped up and were resolved during the experiment. Even with these problems, however, the predicted bounds perform well in terms of correctness.

Table 5.9: Percentage of measurements less than the predicted upper bound for the configuration using the Indiana input source, preemption priority, and UC/ANL resource. For the individual phases (i.e., input, queue, execution, and output), the target quantile was 0.95; for the overall bound, the quantile was 0.815.

Resource	# of Trials	Input	Queue	Execution	Output	Overall
UC/ANL IA-64	109	98%	94%	93%	85%	95%

Table 5.10: The percent overprediction for each phase of the configurations utilizing the Indiana input source, preemption priority and UC/ANL resource.

Resource	Input	Queue	Execution	Output	Overall
UC/ANL IA-64	5.72%	75.08%	4.39%	7.39%	6.45%

In all, the results from this experiment demonstrate the correctness and accuracy of the bounding methodology for the preemption priority. Similar to the next-to-run priority, this priority mechanism greatly reduces the overprediction seen with normal priority. And, as one would expect, the preemption policy provides a lower average delay (10,350 seconds) and lower average composite bound (11,019 seconds) than the next-to-run priority—despite the fact that all jobs in the preemption experiment had a non-trivial batch queue delay. However, this delay was much less variable than in the next-to-run experiment. This result supports the hypothesis that as the elevated priority increases, the average delay will decrease with correspondingly tighter upper bounds.

5.5 Experiment 5: Overlapping Input and Resource Allocation Phases

The purpose of the fifth experiment was to determine the significance of the benefit gained from overlapping the input file staging phase with the resource allocation phase. The benefit is an increase in the composite quantile with a lower corresponding bound. This experiment targeted the 0.95 quantile for the queue, execution, and output phases. However, because the queue bounds were so conservative, the 0.9995 quantile for the input phase was used. As a result, the composite quantile for the overlapped phases is 0.9995 * 0.95 = 0.949, which results in the 0.857 overall quantile. From a practical standpoint, the job had to be able to handle the situation where it began execution but the input data was not yet available. For this experiment, the job was modified so that it would "spin" until the data was available. These experiments were conducted on the configuration that consisted of the Indiana input source, the Mercury resource, and normal priority. Because an execution history of 200 runs was now available for Mercury, the execution delay was emulated by randomly sampling the execution history after the input data was available. In addition, the requested wall clock time was also increased in order to account for the potential extra execution time. For these experiments, the wall clock time was increased by the bound corresponding to the upper 0.95 quantile for the input phase. This modification could potentially place the job into a new group for the QBETS tool. However, this experiment tracked the predicted bounds for both the original requested wall clock time and the modified wall clock time, and they were equal.

The predicted bounds plotted against the actual delays are shown in Figure 5.4, and the results of the probabilistic bounds are summarized in Table 5.11. In all, 102 trials of this configuration were completed. In this experiment, all of the phases met the targeted success rate of 95% except for the output phase, which had a success rate of 92%. However, this had little impact on the overall success rate: all 102 trials finished with a delay less than the upper bound. Also, the overlapped input and queue phases all met the combined upper bound for these two phases. In this case, the upper bound for the batch queue was so conservative that it always served as the upper bound for the overlapped phases. The gain was that the bound for the input phase (which was now the 0.9995 quantile rather than the 0.95) was subsumed by the batch queue bound. In this experiment, the typical savings was 1,600 seconds in the composite bound.

Table 5.11: Percentage of measurements less than the predicted upper bound for the configuration using the Indiana input source, normal priority, and overlapping input and queue phases on the Mercury resource. For the queue, execution, and output phases, the target quantile was 0.95; for the overlapped input phase, the target quantile was 0.9995; for the overall bound, the quantile was 0.857. There were a total of 102 trials.

Resource	Input	Queue	Overlapped I&Q	Execution	Output	Overall
Mercury	100%	100%	100%	96%	92%	100%

The overprediction percentage for each phase is listed in Table 5.12. As in previous experiments, the batch queue delay in the normal priority accounts for the conservativeness of the overall bound. However, by overlapping the input and queue phase, some of this conservativeness is absorbed by the actual input delay. The overall overprediction rate is actually higher than in the normal priority experiment. However, the overprediction rate for the batch queue phase in this experiment is also four times larger than the rate in the normal priority experiment for Mercury. The benefit from overlapping the phases is evidenced by the fact that the overprediction

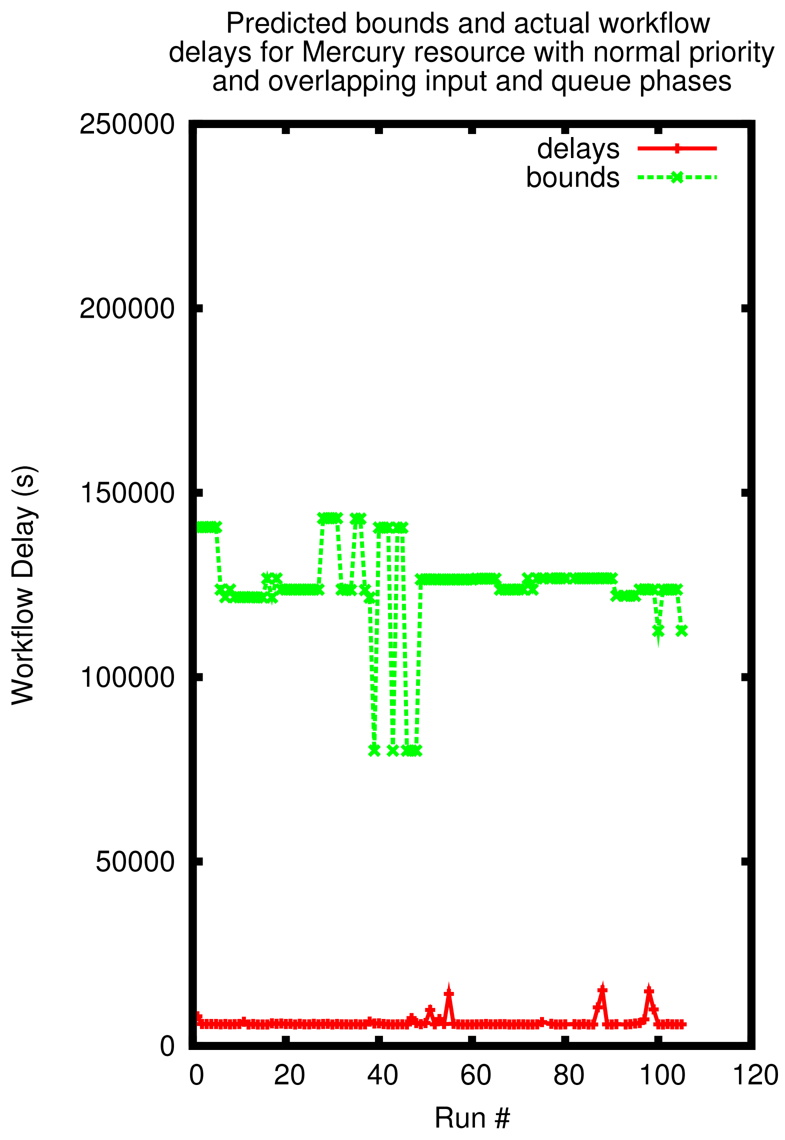

Figure 5.4: Predicted upper 0.857 quantile versus the actual delay achieved by the configuration using the Indiana input source, normal priority, and overlapping input and queue phases for the Mercury resource.

rate for the overlapped phases is less than half the rate for the queue phase (as seen in Table 5.12). In this experiment, the average trial lasted 6,362 seconds, whereas the average bound was 124,906 seconds.

Table 5.12: Percent overprediction for each phase of the configuration using the Indiana input source, normal priority and overlapping input and queue phases.

Resource	Input	Queue	Overlapped I&Q	Execution	Output	Overall
Mercury	18.68%	15,117%	6,480%	3.15%	3.52%	1,863%

This experiment demonstrated the potential savings possible by overlapping the queue and input phases. In general, the phase with a lower bound is subsumed by the other phase. This savings had little effect in this experiment where the vast overprediction of the batch queue phase overshadowed the overlap. However, a similar approach should be applicable to the configurations using the elevated SPRUCE priorities. Such experiments should be included in future work.

5.6 Experiment 6: Advisor - Approximately Optimizing the Quantile

While the previous experiments explored the correctness and accuracy of the bounds, they also highlighted their conservative nature, particularly in the case of the batch queue bounds for the normal priority. This, in part, was due to the fact that the experiments considered the upper 0.95 quantile for each individual phase. However, it is possible to query other quantiles from each of the bounds generators and determine an approximately optimal probability that a given configuration will meet the deadline (as described in Section 4.5). For this experiment, the following quantiles were predicted for each phase:

- Input: [0.9995, 0.999, 0.9975, 0.995, 0.99, 0.975, 0.95, 0.90]

- Queue: [0.95, 0.75, 0.50]
- Execution: [0.99, 0.90, 0.80, 0.70 ,0.60, 0.50]
- Output: [0.9995, 0.999, 0.9975, 0.995, 0.99, 0.975, 0.95, 0.90]

Thus, there were a total of 1,152 possible combinations to create a composite upper bound with a quantile that ranged from 0.20 to 0.94. Every hour for over 11 days, the predicted quantiles were queried from the various bounds predictors. Then, the possible combinations were considered to determine the highest quantile corresponding to a bound that was less than the deadline. In this experiment, no configurations were executed—this experiment served only to illustrate how the bounds change over time and what the highest quantile for the total turnaround time was for each configuration. In Figure 5.5, the best and worst quantiles are plotted for each of the configurations consisting of the Indiana input source. These quantiles are calculated as either the product of the highest quantiles of each individual phase or the product of the lowest available quantiles. Thus, the composite upper 0.94 and upper 0.20 quantiles are plotted for each configuration. First, in most of the plots a small gap occurs from runs 53 through 80 where there was a problem with the batch queue predictors returning an error. Thus, there is no data for these runs. However, the preemption plot does not include this gap because it generates its predictions from a local bounds generator rather than from the QBETS service.

In Figure 5.5, the variability in the normal priority configurations is apparent (note the different scales in each plot). Similar to the previous experiments, the upper 0.94 quantile for the UC/ANL configuration with normal priority exhibits a bias in the latter half of the plot. The reason is that this experiment was conducted while the preemption experiments were being conducted. Thus, the batch queue bounds began reflecting the performance of those experiments. The large differences exhibited in the normal priority configurations are driven by the batch queue predictions. By

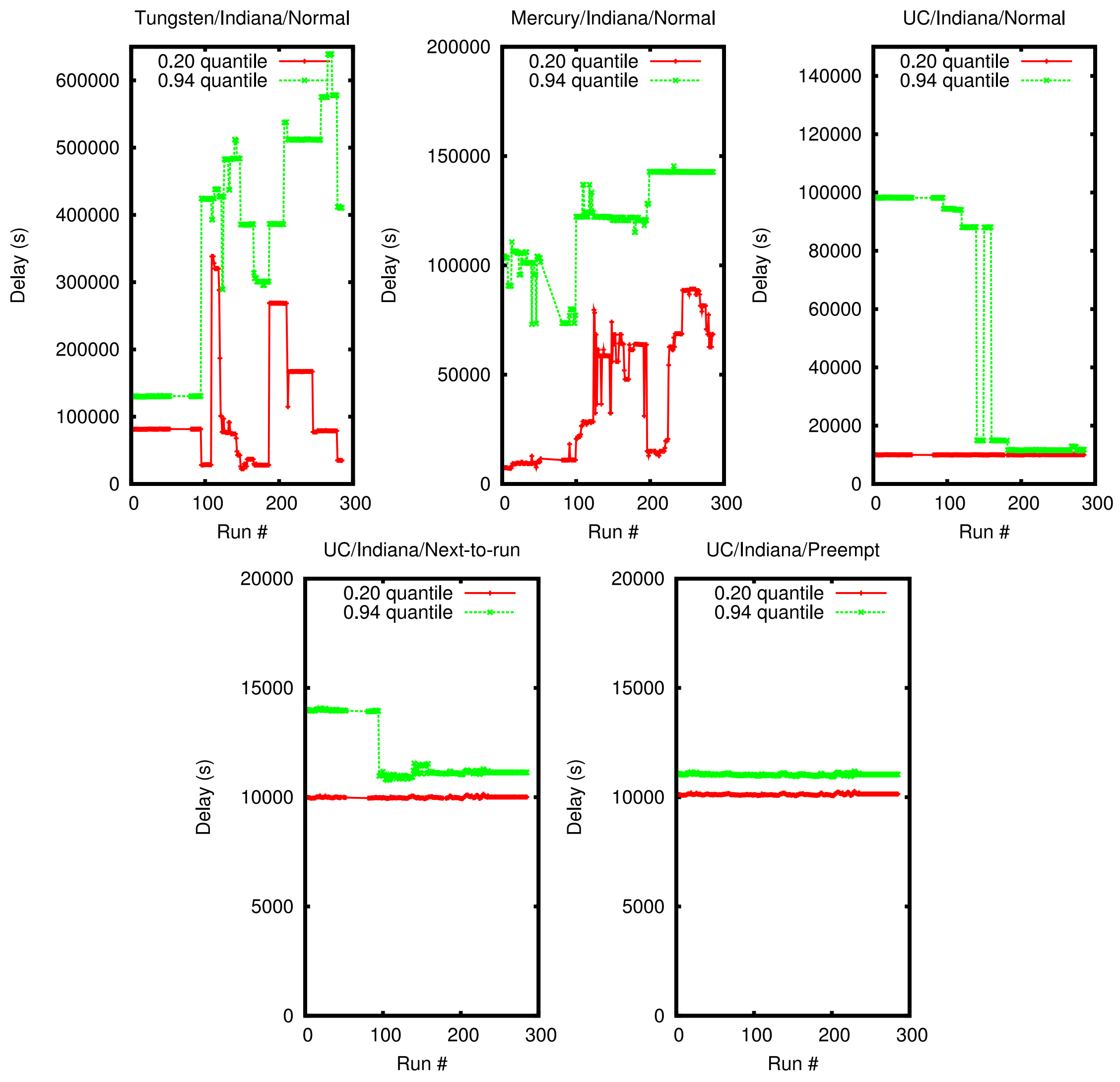

Figure 5.5: Composite bounds of 0.94 and 0.20 for various configurations.

dropping the batch queue quantile from 0.95 to 0.50, there is a very substantial drop in the corresponding bound. Of interest are the plots for the elevated priorities (i.e., next-to-run and preemption). In these two plots, the bounds are not only significantly lower than the normal priority for the UC/ANL resource but also much tighter and with less variability over time. These results are evidence that the elevated priority mechanisms are having their intended effect on the composite total turnaround times. Namely, that they provide SPRUCE users with a much tighter upper bound than the bound for a normal priority job.

Again, the purpose of the Advisor is to maximize the probability that a configuration will meet a given deadline. In Figure 5.6, this was done for the given configurations using a deadline of six hours. In the plot, the highest probability for a bound that is less than six hours is depicted for three configurations: Mercury/Indiana/normal, UC/Indiana/normal, and UC/Indiana/next-to-run. The Tungsten configuration was not pictured because it was unable to generate a bound less than the deadline in any of the trials. Similarly, the preemption configuration for UC/ANL was not depicted because every trial corresponded to the composite 0.94 upper quantile. First, the next-to-run configuration always provides a 94% chance of meeting the six-hour deadline by generating a probabilistic upper bound less than six hours. The normal configuration for the UC/ANL resource has some variability where either a 75% chance of meeting the deadline is reported or a 94% chance. The Mercury configuration exhibits spans of time where no possible combination of individual phase quantiles result in a composite bound less than the deadline. However, there are times when the Mercury configuration has a similar probability of meeting the deadline as the next-to-run configuration. In such a case, a SPRUCE user may decide to submit a job normally rather than spend a token to submit the job as next-to-run. Also, there are times where the next-to-run and preemption configurations both result in a 94% chance of meeting the deadline. In this case, the user may select the next-to-run option rather than unnecessarily killing other jobs that may be executing on the resource.

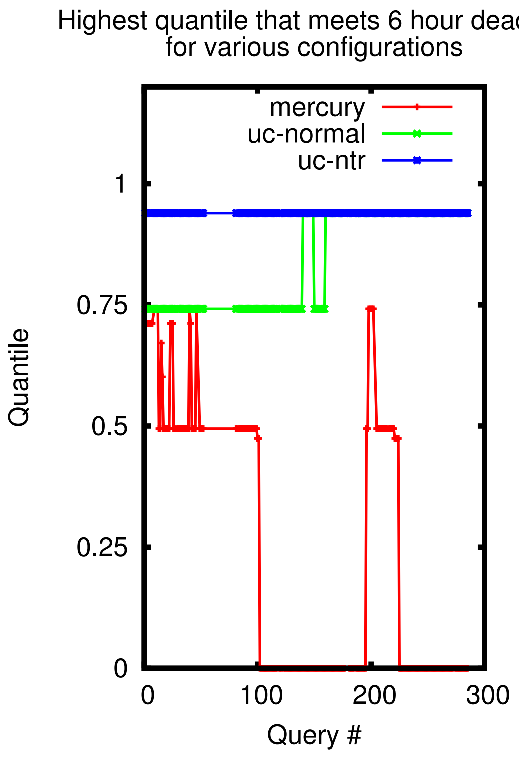

Figure 5.6: Highest quantiles with a bound less than the six-hour deadline for the following configurations: (1) Mercury, Indiana, normal; (2) UC/ANL, Indiana, normal; and (3) UC/ANL, Indiana, next-to-run.

This experiment demonstrates the utility of the simple algorithm implemented by the Advisor to approximate the optimal composite probability by discretizing the quantiles of the individual phases. At a given point of time, each potential configuration has an associated probability of meeting its deadline. If there are multiple configurations with a high probability of success, the user may select the configuration with the less invasive priority (e.g., next-to-run rather than preemption) in an effort to diminish the impact on other users.

Chapter 6

Conclusions

This research has presented a set of methodologies and heuristics that may be used to generate probabilistic upper bounds on the total turnaround time for an urgent computation. These bounds can then be used by the user to select the resource that offers the greatest probability of meeting a given deadline. In the experiments where a normal priority (i.e., no SPRUCE) was used, the variability in batch queue delay clearly results in an overly conservative bound. In the case study, this conservativeness resulted in a composite upper bound that was more than an order of magnitude larger than the actual delay achieved. While such a bound would have little value to an urgent computing user, this behavior is an implicit argument for SPRUCE, which seeks to reduce the amount of time that urgent computations will spend waiting in a batch queue. As a side effect, the bounds generated for these elevated priorities have been shown in the case study to be significantly more accurate while retaining their correctness. However, because the resource allocation bound is generated on previously observed events, it is possible that current queue state can inform the user of situations in which the bounds are overly conservative or when the bounds might be exceeded. In such situations, the user will be able to select an alternative configuration.

This research contributes the first experimentation with the next-to-run batch queue methodology in a Grid resource selection capacity. Moreover, this research is the first to use the BMBP methodology to generate probabilistic upper bounds on execution delay. The case study results indicate that this methodology did a reasonable job in providing both correct and accurate bounds. In addition, the general nature of the tool was highlighted in the case of the UC/ANL resource, which consists of two nodes types with distinct CPU clock speeds. As a result, the execution delays for this resource were bimodal, depending on the nodes that were allocated. The BMBP methodology did not have a problem with this bimodality.

This research also introduces a methodology of creating composite probabilistic bounds based on individual phase bounds generated from several different methodologies. These composite bounds were shown to be correct in all the experiments of the case study and were relatively accurate for the bounds using elevated priorities. As a result, these bounds would provide useful guidance to users in the urgent computing domain.

Chapter 7

Future Work

While the Advisor prototype has generated several interesting results, it has also highlighted several areas for future research. In the immediate future, the next-to-run bounds predictors should be ported to the Mercury and Tungsten resources. Further validation of the tool on larger resources that do not suffer from the underutilization problems of the UC/ANL resource would be beneficial. Also, SPRUCE is currently supported at a number of TeraGrid sites with next-to-run as the policy. Making this tool available for those resources is necessary for the Advisor to be able to compute the composite upper bounds for SPRUCE users.

In addition, the warm standby mechanism that the Advisor relies on needs to be standardized and automated. The mechanism is currently cobbled together by a series of scripts that were used in the case study. In order for the Advisor tool to be offered to SPRUCE users (such as LEAD), this mechanism must be in place.

Another possible future consideration for the Advisor is resource reservations. If an urgent computing user is able to create a reservation on a resource, the uncertainty about when the job will begin execution is eliminated. In this case, the input data may be transferred ahead of time. With regard to the Advisor, the probability of meeting the deadline would now consist only of the execution delay and output file staging. From the case study experiments, these two bounds tended to be both correct and accurate, which would most likely provide the user with a much more useful bound (with less overprediction) without the user having to submit an urgent computation at an elevated priority.

One interesting research project that could be incorporated into the urgent computing model is network provisioning. Gommans, et al. [22] suggest a token-based approach to enable access to connection-oriented network resources. In the SPRUCE model, once a token is activated for urgent computation, one could also allocate the necessary data transport facilities to ensure data transfer at maximum bandwidth. For the Advisor, reserving network bandwidth would affect the file staging phases. Not only would such a reservation increase the average bandwidth for file staging, but it would also most likely decrease the variability. With this modification, the Advisor would need to be able to periodically monitor the bandwidth for a reserved network path.

References

[1] C. D. Keeling, R. B. Bacastow, and T. P. Whorf, "Measurements of the concentration of carbon dioxide at Mauna Loa Observatory, Hawaii", *Carbon Dioxide Review*, pp. 377 – 385, 1982.

[2] K. Nagel, R. Beckman, and C. Barrett, "Transmins for transportation planning", in *6th Int. Conf. on Computers in Urban Planning and Urban Management*, 1999.

[3] Pete Beckman, Suman Nadella, Nick Trebon, and Ivan Beschastnikh, "Spruce: A system for supporting urgent high-performance computing", in *IFIP WoCo9 Conference Proceedings (to appear)*, 2006.

[4] "Spruce: Urgent computing for supercomputers", http://spruce.uchicago.edu.

[5] Jarek Nabrzyski, Jan Weglarz, and Jennifer M. Schopf, *Grid Resource Management: State of the Art and Future Trends*, chapter 2, pp. 15–24, Springer, 2003.

[6] Beulah Kurian Alunkal, Ivana Veljkovic, Gregor von Laszeqski, and Kaizar Amin, "Reputation-based grid resource selection".

[7] Douglas Thain, Todd Tannenbaum, and Miron Livny, "Condor and the Grid", in *Grid Computing: Making the Global Infrastructure a Reality*, Fran Berman, Geoffrey Fox, and Tony Hey, Eds. John Wiley & Sons Inc., December 2002.

[8] R. Raman, M. Livny, and M. Solomon, "Matchmaking: Distributed resource management for high throughput computing", *hpdc*, vol. 00, pp. 140, 1998.

[9] C. Liu, L. Yang, I. Foster, and D. Angulo, "Design and evaluation of a resource selection framework for Grid applications", *High Performance Distributed Computing, 2002. HPDC-11 2002. Proceedings. 11th IEEE International Symposium on*, pp. 63–72, 2002.

[10] Rajkumar Buyya, David Abramson, Jonathan Giddy, and Heinz Stockinger, "Economic models for resource management and scheduling in grid computing",

Concurrency and Computation: Practice and Experience, vol. 14, pp. 1507–1542, 2002.

[11] Daniel Nurmi, Anirban Mandal, John Brevik, Chuck Koelbel, Rich Wolski, and Ken Kennedy, "Evaluation of a Workflow Scheduler Using Integrated Performance Modelling and Batch Queue Wait Time Prediction", *SuperComputing Conference*, 2006.

[12] John Brevik, Daniel Nurmi, and Rich Wolski, "Predicting bounds on queuing delay for batch-scheduled parallel machines", in *PPoPP '06: Proceedings of the eleventh ACM SIGPLAN symposium on Principles and practice of parallel programming*, New York, NY, USA, 2006, pp. 110–118, ACM Press.

[13] A. Mandal, K. Kennedy, C. Koelbel, G. Marin, J. Mellor-Crummey, B. Liu, and L. Johnsson, "Scheduling Strategies for Mapping Application Workflows onto the Grid", *IEEE International Symposium on High Performance Distributed Computing (HPDC 2005)*, 2005.

[14] Rich Wolski, "Experiences with predicting resource performance on-line in computational grid settings", *SIGMETRICS Perform. Eval. Rev.*, vol. 30, no. 4, pp. 41–49, 2003.

[15] "TeraGrid", http://www.teragrid.org/index.php.

[16] M. Allen, J. Brevik, and R. Wolski, "Comparing network measurement time-series", in *MetroGrid Workshop*, October 2007.

[17] Daniel Nurmi, John Brevik, and Rich Wolski, "QBETS: Queue bounds estimation from time series", In Press.

[18] J. Schopf, M. D'Arcy, N. Miller, L. Pearlman, I. Foster, and C. Kesselman, "Discovery in a web service framework: Functionality and performance of the globus toolkits mds4", Technical Report ANL/MCS-P1248-0405, Argonne National Laboratory, 2005.

[19] B. Fryxell, M. Zingale, FX Timmes, DQ Lamb, K. Olson, AC Calder, LJ Dursi, P. Ricker, R. Rosner, JW Truran, et al., "Numerical simulations of thermonuclear flashes on neutron stars", *Nuclear Physics A*, vol. 688, no. 1, pp. 172–176, 2001.

[20] "LEAD Portal", https://portal.leadproject.org/gridsphere/gridsphere.

[21] S. Marru, D. Gannon, S. Nadella, P. Beckman, D.B. Weber, K.A. Brewster, and K.K. Droegemeier, "Lead cyberinfrastructure to track real-time storms using spruce urgent computing", *CTWatch Quarterly*, vol. 4, March 2008.

[22] Leon Gommans, Franco Travostino, John Vollbrecht, Cees de Laat, and Robert Meijer, "Token-based authorization of connection oriented network resources", in *GRIDNETS*, October 2004.